

Critical microwave-conductivity fluctuations across the phase diagram of superconducting $\text{La}_{2-x}\text{Sr}_x\text{CuO}_4$ thin films

Haruhisa Kitano,¹ Takeyoshi Ohashi,¹ Atsutaka Maeda,¹ and Ichiro Tsukada²

¹*Department of Basic Science, University of Tokyo, 3-8-1, Komaba, Meguro-ku, Tokyo 153-8902, Japan*

²*Central Research Institute of Electrical Power Industry, 2-11-1, Iwadokita, Komae, Tokyo 201-8511, Japan*

(Received 10 January 2006; published 13 March 2006)

We report a systematic study of the dynamic microwave conductivity near T_c for $\text{La}_{2-x}\text{Sr}_x\text{CuO}_4$ (LSCO) thin films with $x=0.07-0.16$. The strong frequency dependence of the phase stiffness together with scaling analysis of the ac fluctuating conductivity of superconductivity provide direct evidence for the two-dimensional-XY behavior of nearly decoupled CuO_2 planes in underdoped LSCO ($x=0.07$ and 0.12). On the other hand, the critical exponents for slightly overdoped LSCO ($x=0.16$) were found to agree with those for the relaxational three-dimensional-XY model, indicating that the universality class in LSCO is changed by hole doping. The implication of these results for the phase diagram of high- T_c cuprates is discussed.

DOI: [10.1103/PhysRevB.73.092504](https://doi.org/10.1103/PhysRevB.73.092504)

PACS number(s): 74.25.Nf, 74.40.+k, 74.72.Dn, 74.78.Bz

One of the hallmarks of the high- T_c cuprates is the large thermal fluctuation of the superconducting order enhanced by the short coherence length and the quasi-two-dimensionality, which enables the exploration of the fluctuation-dominated critical regime very close to T_c .¹ Although numerous measurements, such as the ac conductivity,² the dc magnetization,³ the specific heat,⁴ and the I - V curves,⁵ have been performed to investigate the critical fluctuation, there has been no consensus among the results. This is surprising because the critical phenomena were considered to be universal, independent of the microscopic details.⁶ However, if many assumptions were made implicitly to determine the universality class of the phase transition from the data, the obtained results are not convincing unless the validity of such assumptions is confirmed. Thus one should develop a more reliable method which does not require any extra assumptions. To our knowledge, the most successful method is dynamic scaling analysis of the ac complex conductivity, $\sigma(\omega)=\sigma_1(\omega)-i\sigma_2(\omega)$, as will be discussed later.

Another fascinating hallmark of the high- T_c cuprates is that the physical properties change with hole doping. In particular, an understanding of the phase diagram as a plot of T_c versus the hole concentration has been a central issue in the physics of high- T_c cuprates. Interestingly, some recent models, which start from the quantum criticality for competing orders underlying the phase diagram of high- T_c cuprates, provide another possible explanation for the critical fluctuations in high- T_c cuprates. That is, the critical fluctuations change with hole doping because of the existence of a quantum critical point (QCP).⁷ These models suggest that the critical dynamics should be investigated as a function of hole doping. Thus it can be expected that such a systematic study across the phase diagram will not only resolve the disagreements among earlier studies but will also provide important information to understand the phase diagram of high- T_c cuprates.

In this paper, we report a systematic study of $\sigma(\omega)$ as a function of the swept-frequency (0.1–12 GHz) for high-quality $\text{La}_{2-x}\text{Sr}_x\text{CuO}_4$ (LSCO) thin films with a wide range

of hole concentrations ($x=0.07-0.16$). For underdoped (UD) LSCO, we show clear evidence for the two-dimensional (2D)-XY critical fluctuation of nearly decoupled CuO_2 planes. With increasing hole doping, a dimensional crossover from 2D-XY behavior to three-dimensional (3D)-XY behavior was observed near $x=0.16$, implying that there are at least two universality classes in the phase diagram of LSCO.

Epitaxial LSCO thin films with $x=0.07$, 0.12 (underdoped), 0.14 (nearly optimally doped), and 0.16 (overdoped) were grown on LaSrAlO_4 (001) substrates by a pulsed laser deposition technique using pure ozone.⁸ All the films are highly c -axis oriented with a sufficiently narrow rocking curve of the 002 reflection (typically 0.2°). As shown in Table I, the value of the in-plane dc resistivity, ρ_{dc} , was found to agree with the reported best value for LSCO thin films⁹ within a factor of 2, confirming that the films used in this study are of sufficiently high quality to investigate the critical dynamics near T_c .

There are three reasons for using LSCO films on LaSrAlO_4 (LSAO) substrates in this study: (1) LSCO is an ideal system with a simple layered structure, where the hole concentration can be widely controlled. (2) The compressive epitaxial strain gives rise to a moderate increase of T_c .⁹ (3) The tetragonal symmetry of LSAO substrate supports the fabrication of CuO_2 planes with ideal flat square lattices, free from disorders due to corrugations and twin boundaries.⁸

Both the real and imaginary parts of $\sigma(\omega)$ were obtained from the complex reflection coefficient, $S_{11}(\omega)$, using a non-

TABLE I. Values of t , ρ_{dc} , and T_c for the measured films. ρ_{dc} is the value at $T=50$ K. As for three kinds of T_c , see the text for definition.

x	t (nm)	ρ_{dc} (m Ω cm)	T_c^{scale} (K)	T_c^0 (K)	T_{MF} (K)
0.07	460	0.77	19.0	20.83	~ 32
0.12	230	0.28	33.65	36.08	~ 38
0.14	270	0.14	38.92	39.29	~ 40
0.16	140	0.12	35.5	35.82	

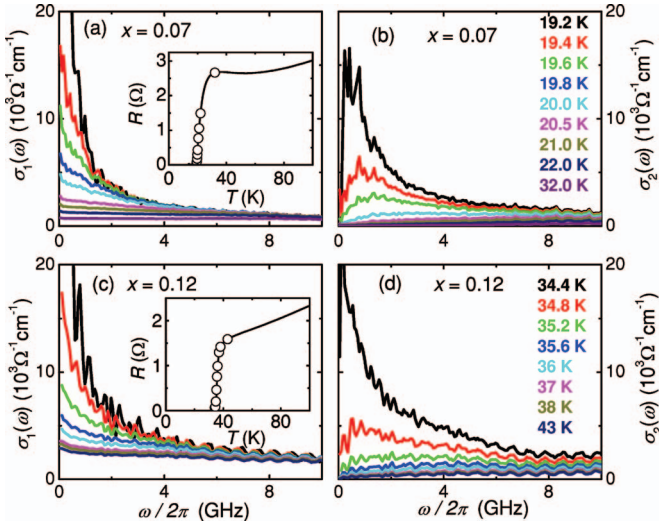


FIG. 1. (Color) The frequency dependence of (a) $\sigma_1(\omega)$ for $x=0.07$, (b) $\sigma_2(\omega)$ for $x=0.07$, (c) $\sigma_1(\omega)$ for $x=0.12$, and (d) $\sigma_2(\omega)$ for $x=0.12$, respectively. Insets: the temperature dependence of the dc resistance, R , of the same sample. Open circles near T_c show R at the temperatures presented in the main panel.

resonant broadband technique.¹⁰ When the film thickness, t , is sufficiently less than the skin depth, δ , one can write $\sigma(\omega)$ as follows:

$$\sigma(\omega) = \frac{1}{t} \frac{1 - S_{11}(\omega)}{Z_0(1 + S_{11}(\omega))}, \quad (1)$$

where $Z_0=377 \Omega$ is the impedance of free space. In practice, before applying Eq. (1), systematic errors involved in $S_{11}(\omega)$ were carefully removed by calibration measurements using known standards.¹⁰

In order to obtain reliable $\sigma(\omega)$ data, the effect of the dielectric substrate needs to be considered. Note that the choice of t according to values of ρ_{dc} is important because a resonance peak attributed to the effect of substrate can be induced for a very small value of t .¹¹ In fact, a sharp resonance peak has been observed near 8 GHz for the LSCO film ($x=0.07$) above 100 K.¹⁰ However, in the data presented in Fig. 1, no peak was observed over the whole frequency range measured at lower temperatures near T_c . Thus we can conclude that the effect of substrate was negligible near T_c .

Moreover, in the vicinity of T_c , we found that $\sigma(\omega)$ was seriously affected by a small unexpected difference (typically, 0.2° to 0.3° at 1 GHz) between the phase of S_{11} for a load standard, $\angle S_{11}^{\text{load}}$, and that for a short standard, $\angle S_{11}^{\text{short}}$. This difficulty was resolved by using the measured $S_{11}(\omega)$ of the sample at a temperature far above T_c as the load standard, assuming that $\angle S_{11}^{\text{short}} = \angle S_{11}^{\text{load}}$ at this temperature, and that both were T -independent in the vicinity of T_c . The validity of this procedure was also confirmed by the same measurements for NbN thin films as a reference.¹²

Figure 1 shows the frequency dependence of $\sigma(\omega)$, obtained by the above procedures, for underdoped LSCO ($x=0.07$ and 0.12) at several temperatures above T_c . It is evident that both $\sigma_1(\omega)$ and $\sigma_2(\omega)$ diverge rapidly with decrease-

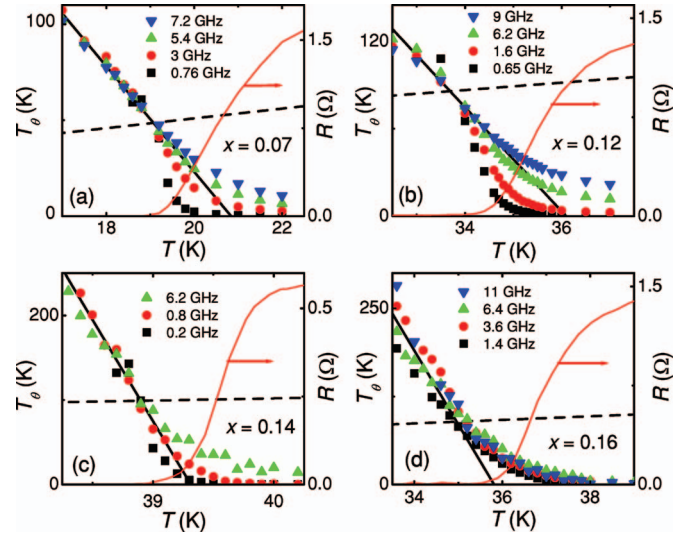


FIG. 2. (Color) The phase-stiffness temperature for the film with (a) $x=0.07$, (b) $x=0.12$, (c) $x=0.14$, and (d) $x=0.16$. The dashed straight line represents $(8/\pi)T$. The solid straight line gives the bare phase stiffness in the XY model, while it gives the mean-field superfluid density in the GL theory. In each panel, the dc resistance was given by red solid curves.

ing temperature in the low frequency limit, suggesting that the excess conductivity is due to the superconducting fluctuations. A similar divergence in $\sigma(\omega)$ was also observed in the vicinity of T_c for the other LSCO films.

It has been argued¹³ that strong phase fluctuations are important for the determination of T_c in the UD region because the phase-stiffness energy, $k_B T_\theta \equiv (\hbar/e^2)\hbar\omega\sigma_2 d_s$, is suppressed largely by the small superfluid density, where d_s is the effective thickness of a superfluid. Figure 2 shows the phase-stiffness temperature $T_\theta(T)$ estimated from $\sigma_2(\omega, T)$ at several frequencies. Surprisingly, we found that $T_\theta(T)$ for the UD samples ($x=0.07$ and 0.12) started to show frequency dependence above a certain temperature, T_k , while $T_\theta(T)$ was almost ω -independent below T_k . In addition, the resistive T_c (T_c^R), where R became zero, was also close to T_k rather than another critical temperature, T_c^0 , where the bare phase stiffness in the XY model would go to zero. When we assumed d_s to be approximately $t/2$, we saw that a dashed straight line with a slope of $8/\pi$ crossed $T_\theta(T)$ at T_k , indicating that T_k agrees with the Berezinskii-Kosterlitz-Thouless (BKT) transition temperature, T_{BKT} , in the 2D-XY model.^{14,15}

As shown in Figs. 2(c) and 2(d), this behavior was observed even for $x=0.14$, while it disappeared almost completely for $x=0.16$. T_c^R for $x=0.16$ was close to T_c^0 rather than T_{BKT} , suggesting that the mean field critical temperature T_{MF} is close to T_c^0 . Thus our results were qualitatively similar to the prediction of Emery and Kivelson¹³ in the sense that T_c is bounded by T_{BKT} (UD region) or T_{MF} (overdoped region), although the estimation of T_{MF} in the UD region was considerably different, as will be discussed later.

In the dynamic scaling analysis of the fluctuating complex conductivity, $\sigma_{\text{fl}}(\omega)$, which was pioneered by Booth *et al.*,² both the magnitude, $|\sigma_{\text{fl}}|/\sigma_0$, and the phase, $\phi_\sigma (\equiv \tan^{-1}[\sigma_2^{\text{fl}}/\sigma_1^{\text{fl}}])$, of $\sigma_{\text{fl}}(\omega)$ are used as scaled quantities.

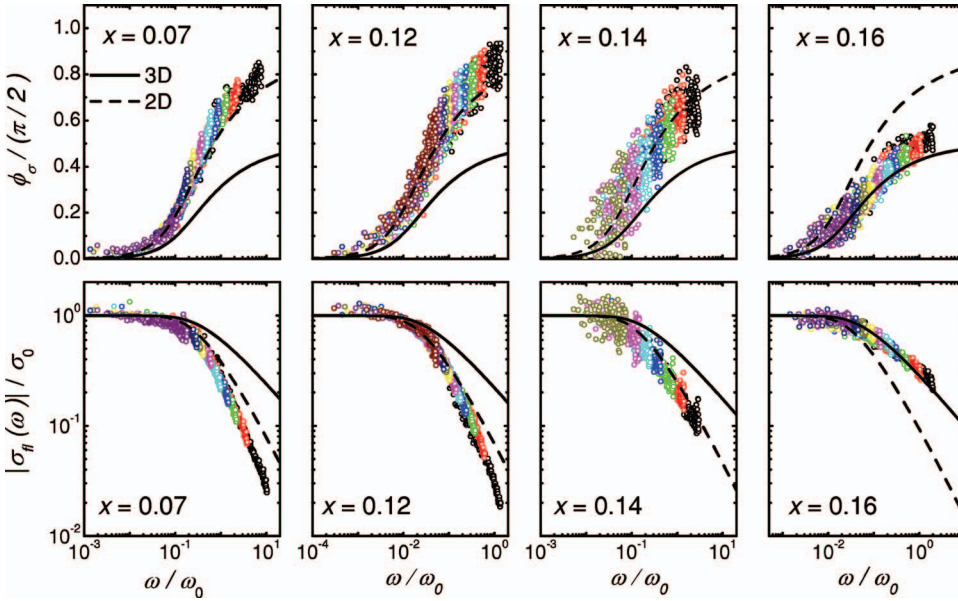


FIG. 3. (Color) Scaled curves of ϕ_σ (upper panels) and $|\sigma_\Pi|$ (lower panels) for the measured LSCO film. $\sigma_\Pi(\omega)$ was obtained by subtracting the normal-state conductivity at 32 K ($x=0.07$), 38 K ($x=0.12$), and 40 K ($x=0.14, 0.16$), respectively. Data for $x=0.07$ span the frequency range 0.2–7 GHz at reduced temperatures $\epsilon=0.01$ –0.5, while those for $x=0.16$ span 0.2–2 GHz at reduced temperatures, $\epsilon=0.002$ –0.08. The solid (dashed) lines are the 3D (2D) Gaussian scaling functions.

The advantage of this method is that the data collapse to a single curve as a function of a reduced frequency, ω/ω_0 , can be achieved without assuming any relationship between two scaling parameters, σ_0 and ω_0 , in contrast to other scaling analyses.^{3–5} Note that σ_0 and ω_0 are obtained independently in our analysis. Thus we can begin by checking the following hypothesis of the dynamic scaling theory,¹

$$\sigma_\Pi(\omega) \approx \xi^{z+2-d} S(\omega\xi^z), \quad (2)$$

where $S(x)$ is a complex universal scaling function, ξ is a correlation length which diverges at T_c , z is a dynamic critical exponent, and d is an effective spatial dimension. Figure 3 shows that both $|\sigma_\Pi|/\sigma_0$ and ϕ_σ were scaled successfully over a wide range of frequencies for all the films, confirming that the critical dynamics suggested by Eq. (2) were indeed observed. The comparison of the experimentally obtained scaling functions with the Gaussian forms calculated by Schmidt¹⁶ suggested that the 2D Gaussian-like behavior in the UD region changed into the 3D Gaussian-like behavior near $x=0.16$.

Equation (2) suggests that both σ_0 and ω_0 behave as functions of ξ in a critical region, where $\sigma_0 \propto \xi^{z+2-d}$ and $\omega_0 \propto \xi^{-z}$. According to the BKT theory,^{14,15} ξ_{KT} diverges with $\exp[b/\sqrt{\epsilon}]$ in the critical region, $T_c < T \ll T_c^0$, where $\epsilon \equiv T/T_c^{\text{scale}} - 1$ and b is a numerical constant. Note that $\sigma_0 = 1/\omega_0 \propto \xi^2$ for the relaxational 2D system with $z=2$.¹ In fact, we confirmed that both σ_0 and ω_0 for $x=0.07$ showed the same exponential singularity as ξ_{KT}^2 with $b=0.215$ in the range of ϵ from 0.01 to 0.1, as shown in Figs. 4(a) and 4(b). With increasing x up to 0.14, we found that the range of ϵ where σ_0 (or ω_0) agreed with ξ_{KT}^2 became narrower and shifted to lower temperatures. Such behaviors were also consistent with the BKT theory,¹⁵ since σ_0 (or ω_0) is rather dominated by free vortices than ξ_{KT}^2 at higher temperatures, due to a screening effect by thermally activated free vortices.

In the BKT theory, $\sigma_0\omega_0$ gives T_θ in the high-frequency limit, T_θ^0 , which is sensitive to the surviving bound pairs of vortices above T_{BKT} .¹⁵ As shown in Fig. 4(c), we found that

$\sigma_0\omega_0$ decreased with increasing T more quickly at larger x . This suggests that the temperature region of the prominent phase fluctuation became narrower with hole doping, in contrast to a recent Nernst experiment¹⁷ which showed a steeper increase of the onset temperature of the Nernst effect than T_c with increasing hole doping. When we roughly estimated T_{MF} , based on an expectation that $\sigma_0\omega_0 \approx 0$ at T_{MF} , we found that T_{MF} was too small to cover the pseudogap region, as was

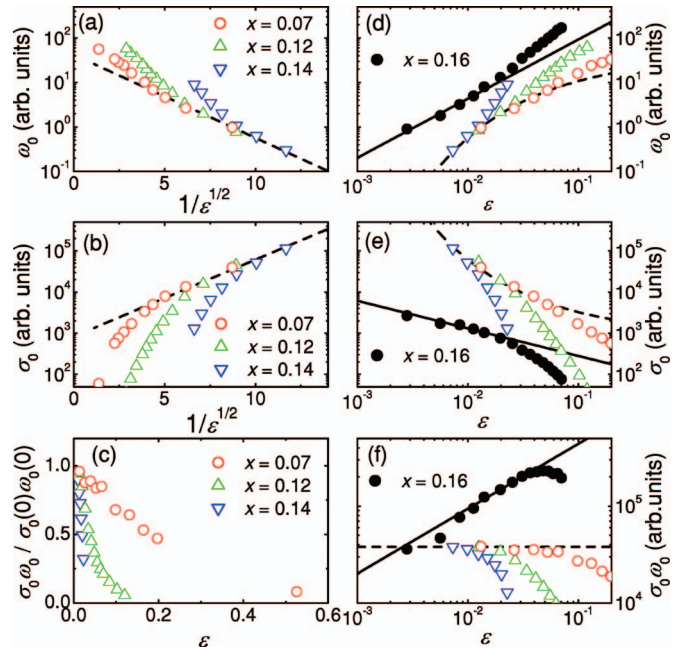


FIG. 4. (Color) (a) ω_0 and (b) σ_0 as a function of $1/\sqrt{\epsilon}$ for $x=0.07$ –0.14, where $\epsilon=T/T_c^{\text{scale}}-1$. The dashed line is (a) ξ_{KT}^{-2} and (b) ξ_{KT}^2 . (c) $\sigma_0\omega_0$ vs ϵ for $x=0.07$ –0.14. (d) ω_0 , (e) σ_0 , and (f) $\sigma_0\omega_0$ as a function of ϵ for $x=0.07$ –0.16. The solid line is (d) $\epsilon^{1.33}$, (e) $\epsilon^{-0.67}$, and (f) $\epsilon^{0.67}$. The dashed line is (d) ξ_{KT}^{-2} , (e) ξ_{KT}^2 , and (f) the behavior expected in $d=2$. Note that the absolute values of the plots in all the panels except for (c) are unimportant, since they include arbitrary proportional coefficients.

previously reported by Corson *et al.*² These results strongly suggested that most of the anomalous Nernst signal should be attributed to other origins than the superconducting fluctuation, as was suggested by some recent theoretical works.¹⁸

Moreover, the observed reduction of T_c due to the phase fluctuation ($T_{\text{BKT}}/T_{\text{MF}} \sim 0.7, 0.9$ for $x=0.07, 0.12$, respectively) corresponded to the superconducting film with a very high sheet resistance $R_{\text{sq}} (\sim 3-5 \text{ k}\Omega)$.¹⁹ Using a relation $R_{\text{sq}} = \rho_{\text{dc}}/D_s$, we found that $D_s \sim 10 \text{ \AA}$. Thus each of the CuO_2 planes seemed to be decoupled.^{1,20} Note that the screening length for each superconducting sheet, $\lambda_{\perp} (= \lambda^2/D_s)$, where λ is a bulk penetration depth, was larger than 10 nm in this case, which satisfied the BKT criterion that $\lambda_{\perp} \gg L$, where L is the sample size. In addition, d_s is given by a sum of the decoupled superconducting layers with the thickness of D_s . Thus d_s will be smaller than t , as we assumed in the estimation of $T_{\theta}(T)$ shown in Fig. 2.

We found that the critical behavior for $x=0.16$ was very different from that for $x=0.07-0.14$, as shown in Figs. 4(d)–4(f). In particular, the dimensionality of $x=0.16$ was found to be three, in contrast to the 2D-XY behavior of $x=0.07-0.14$, as shown by the plots of $\sigma_0\omega_0 (\propto \epsilon^{\nu(d-2)})$ in Fig. 4(f), where ν is a static critical exponent. We also confirmed that the critical exponents for $x=0.16$ agreed very well with those for the relaxational 3D-XY model with $\nu \approx 0.67$, $z \approx 2$, and $d=3$.²¹ These results clearly suggest that the universality class in the phase diagram of LSCO changes from 2D-XY to 3D-XY with hole doping.

What is the origin of the dimensional crossover from 2D-XY to 3D-XY? One of candidates is the increase of the inter-layer coupling (probably Josephson coupling) with hole doping.^{1,20} However, this effect seems to appear more gradually with hole doping, in contrast to the different behavior

between $x=0.14$ and 0.16 shown in Figs. 3 and 4(f). Another candidate is the effect of the quantum critical fluctuation near QCP. In this case, the 2D-3D crossover can be regarded as the classical-to-quantum crossover near QCP.⁷ A detailed study for further over-doped LSCO is needed to settle this issue.

Finally, we emphasize that all the above results rule out the possibility of the distribution of T_c due to disorders in the sample. If there is a broad distribution of T_c in the sample, σ_2 will be greatly suppressed, leading to a smaller T_{θ} , and the dynamic scaling of $|\sigma|$ and ϕ_{σ} will fail below a certain temperature, suggesting that T_c^{scale} is higher than T_c^R . In fact, these features have been observed for NbN films with a non-negligible distribution of T_c ,¹² while all of the four LSCO films used for this study did not show them, as shown in Figs. 2–4.

In conclusion, a systematic study of the critical dynamics of $\sigma_{\text{H}}(\omega)$ for LSCO thin films with $x=0.07-0.16$ has been performed for the first time. All the results clearly provide evidence for the BKT transition in the nearly decoupled CuO_2 layers of underdoped LSCO. With increasing hole doping, the 2D-XY behavior in the UD region changes into the 3D-XY behavior near $x=0.16$, indicating that the universality class in the phase diagram of LSCO is changed by hole doping.

We thank Y. Kato, H. Fukuyama, and W. N. Hardy for fruitful discussions and comments, S. Anlage and A. Schwartz for technical advice at the early stages of this study, and D. G. Steel and K. Gomez for useful comments on the manuscript. This work was partly supported by the Grant-in-Aid for Scientific Research (13750005, 14340101, and 15760003) from the Ministry of Education, Science, Sports and Culture of Japan.

¹D. S. Fisher, M. P. A. Fisher, and D. A. Huse, Phys. Rev. B **43**, 130 (1991).

²For example, S. Kamal, D. A. Bonn, N. Goldenfeld, P. J. Hirschfeld, R. Liang, and W. N. Hardy, Phys. Rev. Lett. **73**, 1845 (1994); S. M. Anlage, J. Mao, J. C. Booth, D. H. Wu, and J. L. Peng, Phys. Rev. B **53**, 2792 (1996); J. C. Booth, D. H. Wu, S. B. Qadri, E. F. Skelton, M. S. Osofsky, A. Pigue, and S. M. Anlage, Phys. Rev. Lett. **77**, 4438 (1996); J. Corson *et al.*, Nature (London) **398**, 221 (1999); J. R. Waldram, D. M. Broun, D. C. Morgan, R. Ormeno, and A. Porch, Phys. Rev. B **59**, 1528 (1999); K. M. Paget, B. R. Boyce, and T. R. Lemberger, *ibid.* **59**, 6545 (1999).

³For a review, see Q. Li, in *Physical Properties of High Temperature Superconductors V*, edited by D. M. Ginsberg (World Scientific, Singapore, 1996), p. 209.

⁴For example, A. Junod *et al.*, Physica B **280**, 214 (2000); M. V. Ramallo and F. Vidal, Phys. Rev. B **59**, 4475 (1999), and references therein.

⁵For example, D. R. Strachan, C. J. Lobb, and R. S. Newrock, Phys. Rev. B **67**, 174517 (2003), and references therein.

⁶P. M. Chakin and T. C. Lubensky, *Principles of Condensed Matter Physics* (Cambridge Univ. Press, Cambridge, UK, 1995).

⁷S. Sachdev, Science **288**, 475 (2000); M. Vojta, Rep. Prog.

Phys. **66**, 2069 (2003).

⁸I. Tsukada, Phys. Rev. B **70**, 174520(R) (2004).

⁹H. Sato, T. Tsukada, M. Naito, and A. Matsuda, Phys. Rev. B **61**, 12447 (2000).

¹⁰H. Kitano *et al.*, Physica C **412-414**, 130 (2004).

¹¹E. Silva *et al.*, Supercond. Sci. Technol. **9**, 934 (1996).

¹²T. Ohashi *et al.* (unpublished).

¹³V. J. Emery and S. A. Kivelson, Nature (London) **374**, 434 (1995).

¹⁴V. L. Berezinskii, Sov. Phys. JETP **32**, 493 (1970); J. M. Kosterlitz and D. J. Thouless, J. Phys. C **6**, 1181 (1973).

¹⁵B. I. Halperin and D. R. Nelson, J. Low Temp. Phys. **36**, 599 (1979); V. Ambegaokar, B. I. Halperin, D. R. Nelson, and E. D. Siggia, Phys. Rev. B **21**, 1806 (1980).

¹⁶H. Schmidt, Z. Phys. **216**, 336 (1968).

¹⁷N. P. Ong and Y. Wang, Physica C **408-410**, 11 (2004).

¹⁸H. Kontani, Phys. Rev. Lett. **89**, 237003 (2002); C. Honerkamp and P. A. Lee, *ibid.* **92**, 177002 (2004).

¹⁹M. R. Beasley, J. E. Mooij, and T. P. Orlando, Phys. Rev. Lett. **42**, 1165 (1979).

²⁰S. Hikami and T. Tsuneto, Prog. Theor. Phys. **63**, 387 (1980).

²¹R. A. Wickham and A. T. Dorsey, Phys. Rev. B **61**, 6945 (2000).